



Published in final edited form as:

Proc SPIE Int Soc Opt Eng. 2011 March 14; 7962: 79623X-. doi:10.1117/12.877593.

Robust Biological Parametric Mapping: An Improved Technique for Multimodal Brain Image Analysis

Xue Yang^a, Lori Beason-Held^b, Susan M. Resnick^b, and Bennett A. Landman^{a,b,c,*}

^aElectrical Engineering, Vanderbilt University, Nashville, TN, USA 37235

^bNational Institute on Aging, National Institutes of Health, Baltimore, MD, 21224

^cBiomedical Engineering, Vanderbilt University, Nashville, TN, USA 37235

^dBiomedical Engineering, Johns Hopkins University, Baltimore, MD, USA 21218

Abstract

Mapping the quantitative relationship between structure and function in the human brain is an important and challenging problem. Numerous volumetric, surface, region of interest and voxelwise image processing techniques have been developed to statistically assess potential correlations between imaging and non-imaging metrics. Recently, biological parametric mapping has extended the widely popular statistical parametric approach to enable application of the general linear model to multiple image modalities (both for regressors and regressands) along with scalar valued observations. This approach offers great promise for direct, voxelwise assessment of structural and functional relationships with multiple imaging modalities. However, as presented, the biological parametric mapping approach is not robust to outliers and may lead to invalid inferences (e.g., artifactual low p-values) due to slight mis-registration or variation in anatomy between subjects. To enable widespread application of this approach, we introduce robust regression and robust inference in the neuroimaging context of application of the general linear model. Through simulation and empirical studies, we demonstrate that our robust approach reduces sensitivity to outliers without substantial degradation in power. The robust approach and associated software package provides a reliable way to quantitatively assess voxelwise correlations between structural and functional neuroimaging modalities.

Keywords

Structural and Functional relationships in human brain; Biological Parametric Mapping; Robust Regression

1. INTRODUCTION

Structure and function relationships play an important role in developing our understanding of the human brain. These relationships appear to transcend scales, with connectivity dynamics appearing at both a micro- (intra-voxel) and macro-(the whole brain) scales [1].

*bennett.landman@vanderbilt.edu; phone 1 615 322-2338; fax 615 343-5459; <https://masi.vuse.vanderbilt.edu>.

While there is firm evidence that structure shapes neural dynamics and function, the quantitative relationships and how such relationships might be altered in aging and disease remain unclear. [2]

Statistical parametric mapping (SPM) has emerged as a powerful tool to simultaneously study changes within single voxels along with spatial patterns of activity or tissue volume changes [3]. Recently, biological parametric mapping (BPM) [4] has provided a methodology which allows multi-modal images to be analyzed in the same manner that SPM enables regression of images on scalars. However, the existence of outliers can influence the results of a statistical analysis considerably, especially when the sample size is small. In neuroimaging outliers can appear both because of imaging artifacts, data processing anomalies, and also anatomical differences between brains. These anatomical differences are especially problematic because they introduce systematic and highly correlated variation in both regressors and regressands. To deal with outliers, the field of robust statistics has emerged [5]. Herein, we extend the BPM approach to apply a robust estimation method with robust inference by using M-estimates (first introduced in [6]) in place of ordinary least squares regression.

This manuscript is organized as follows. First, we introduce the robust regression theory as well as robust inference. Then we describe how this approach can be used to develop robust BPM. Simulation examples compare the results from original and robust BPM. We close with a discussion of the advantages of robust BPM and the potential opportunities for continued innovation.

2. THEORY

M-estimators are popular robust regression methods [7]. In the ordinary least squares estimates method, it is assumed that each data point has a measurement error that is independently random and has a normal distribution. But when there are outliers, our measurement errors are not normally distributed. M-estimator assumes that the probability of measurement error is: ([8])

$$P(\text{data}|\text{model}) = \prod_{i=0}^{N-1} \left\{ \exp \left[-\rho \left(\frac{y_i - y(x_i|\beta)}{\sigma} \right) \right] \Delta y \right\} \quad (1)$$

where y_i is measurement, $y(x_i|\beta)$ is predicted value based on the model, σ is weight factor, denotes standard deviation, ρ is small fixed factor on each data point.

The ρ function must be chosen appropriately. If $\rho(r) = \frac{1}{2}r^2$, the M-estimate is equal to the Least Squares estimates. In this case, when an outlier occurs, $y(x_i|\beta)$ is pulled towards the

outlier to minimize $\sum_{i=0}^{N-1} \rho \left(\frac{y_i - y(x_i|\beta)}{\sigma} \right)$, which makes the least squares estimates method sensitive to outliers. In robust regression, $\rho(r)$ does not increase or it increases slowly when $r > C$, thus assigning a small weight to outliers which avoids pulling $y(x_i|\beta)$ towards the outlier. Here in, we choose a Bisquare weight function [9]:

$$\rho(r) = \begin{cases} \left(\frac{c^2}{2}\right) \left[1 - \left[1 - \left(\frac{r}{c}\right)^2\right]^3\right] & |r| \leq C \\ \frac{c^2}{2} & |r| > C \end{cases} \quad (2)$$

Where c is the tuning constant, usually the value is chosen for 95% asymptotic efficiency when the distribution of observation error is Gaussian distribution.

We can use the maximum likelihood algorithm to estimate β . We need to maximize $P(\text{data}|\text{model})$, which is equal to minimizing $-\log P(\text{data}|\text{model})$, which minimizes

$$\sum_{i=0}^{N-1} \rho\left(\frac{y_i - y(x_i|\beta)}{\sigma}\right) \quad (3)$$

Using maximum likelihood method, β should satisfy

$$\sum_{i=0}^{N-1} \rho' \left(\frac{y_i - y(x_i)}{\sigma}\right) \left(-\frac{1}{\sigma}\right) \left(\frac{dy(x_i|\beta)}{d\beta}\right) = 0 \quad (4)$$

To solve this equation, we can use the iteratively reweighted least squares techniques developed in [10], which can be applied to the general linear model (GLM). A specific algorithm to compute the estimated solution of β is provided in [11].

The usual formulas for statistical inference are not meaningful when computed using robust regression. Recently, many robust inference methods have been developed. Huber ([12]) has provided a method to calculate robust covariance:

$$\text{cov}(\hat{\beta}) = K^2 \frac{\left[\frac{1}{n-m}\right] \sum \Psi(r_i)^2}{\left[\left(\frac{1}{n}\right) \sum \Psi'(r_i)\right]^2} (X^T X)^{-1} \quad K = 1 + \frac{m \text{var}(\Psi'')}{n (E\Psi')^2} \quad (5)$$

The author noted that we can use

$$\frac{\sum w_i x_{ij} x_{ik}}{\left(\frac{1}{n}\right) \sum w_i} \quad (6)$$

in place of $X^T X$. Where n is the number of observation y , and m is the number of independent β parameters. The robust covariance formula is based on the assumption that $1 \ll m \ll n$. Details are discussed in [13], which proved in most cases, for normal errors, the

agreement with Monte Carlo results is up to $\frac{m}{n} = 1/4$. A conservative approach was discussed by [14], when there are not many degrees of freedom for error. It is done by not allowing the robust variance to fall much below the variance of the least squares estimate.

3. METHODS

BPM enables the use of image regressors by solving the general linear model (GLM) with different design matrixes in each voxel. This contrasts with conventional SPM (statistical parametric mapping) which can only use non-image regressors as it uses the same design matrix in every voxel. By choosing “regression” in BPM, we can evaluate one image relative to another set of images. BPM has been shown to work well when outliers are not present [4]. The following simulations explore potential modes of failure.

To illustrate the potential problem with outliers, we created 10 simulated images as imaging regressors and another 10 images as the main modality (regressands). The imaging regressor images were created from one image by adding different noises (SNR = 20, CNR = 8). The main modality images were created from the regressor images by multiplying the signal by 3 within a spherical region and constant outside the region. (i.e., $\beta = 3$ inside the sphere, $\beta = 0$ outside the sphere), with SNR = 50, CNR = 31. To simulate an artifact, one pair of regressor and main modality images was shifted. Then, a $y = \beta x + \mu$ model was used to evaluate correlations between the pairs of simulated images. The null hypothesis of $\beta > 0$ was tested.

To explore the potential of robust regression to resolve this issue, we simulated a simple, single voxel model with and without outliers. A set of 21 observations were simulated with an approximately uniform distribution between 10 and 30 (arbitrary units). First, we created simulated data for robust regression in one voxel 10,000 times using the model:

$$y = \beta x + \eta \quad (6)$$

where β is the association parameter and η is noise variable. We used the GLM to fit the dots with the model:

$$y = \beta x + \beta_0 \quad (7)$$

The p value is estimated based on a T-test with null hypothesis $H_0: c' * \beta = 0$, $c = [0 \ 1]$. We evaluate both robust variance provided in [12] with modified $X^T X$ and weighted robust variance in [14]. The estimates results are displayed in Figure 2. The results from ordinary least squares regression and robust regression are similar when there are no outliers. When $\beta = 2$ and there are outliers, the β estimations from ordinary least squares are incorrect while the β estimations from robust regression are around 2. The p values from least squares are not significant. The p values from robust test which uses robust standard error are very small, which show significance. Some of the p values from robust test which uses weighted robust standard error exhibit significance but some of them do not. When $\beta = 0$ and there are outliers, the β estimations from ordinary least squares are not 0 while the beta estimations from robust regression are around 0. The p values from least squares are significant, which are wrong. The p values from robust test which uses robust standard error are distributed as uniform distribution. The p values from robust test which uses weighted robust standard error are closer to 1 than to 0.

From the simple, single voxel model, we can see that the robust regression and robust variance are not affected by outliers. As for the weighted robust variance we found that the p value is not significant when $\beta = 2$ and there are outliers. It is because the least squares variance increases rapidly if the value of y is large. In the practical environment, the assumption $m \ll n$ should be satisfied. Therefore, we decided to use robust variance introduced by [12]. The robust variance can be used to do T-tests and F-tests. In BPM, we propose replacing ordinary variance by robust variance, and use modified $X^T X$ to reduce the outlier effects.

We tested the nonrobust BPM and the robust BPM using a sub-set of the normal aging study of the BLSA neuroimaging project. Herein, we used data from 20 healthy participants (12 M/8 F, 60-85 y/o at baseline). Each subject was studied annually for eight years. We used T1-weighted MRI data (1.5T, GE Medical Systems, SPGR, $0.9375 \times 0.9375 \times 1.5$ mm, $256 \times 256 \times 124$ field of view) and PET data ($[^{15}\text{O}]$, GE 4096+ scanner, 15 slices of 6.5mm thickness, 60s) from the baseline (year 1) and last (year 9) visits. The data were preprocessed with SPM 5 (<http://www.fil.ion.ucl.ac.uk/spm/software/spm5>). The structure scans were normalized to MNI-space, segmented and smoothed (12 mm Gaussian kernel) to obtain smooth gray matter structure images. PET images were normalized, smoothed (12 mm Gaussian kernel) to MNI-space, and calibrated for global blood flow measurements. The smoothed gray matter structure images were regressed on the PET data using nonrobust BPM and robust BPM to explore the potential for gray matter changes to explain changes in PET activation levels. Differences between estimated model fits and significance levels were plotted.

4. RESULTS

Figure 3 shows the GUI and the flowchart we incorporated in BPM. If the user selects robust regression, we use iteratively reweighted least squares method to do M-estimates, and compute robust variance in the GLM model. Other methods remain the same as the original BPM package.

The results from robust BPM are shown in Figure 4, in comparison to the original BPM method. This model uses one of main modality images and one of the regressor images that shifted to create an outlier. The estimated parameter value is the same when there are no outliers. It shows that the original BPM results in the wrong estimation of the model when outliers are present. For the statistical inference, the test map has threshold at $p = 0.0001$ and we can see clearly that almost all voxels inside the designed spherical region have significance while the voxels outside the region do not show significance.

In the results of empirical data, significant effects for each contrast were based on uncorrected p value thresholded at 0.001. We overlap one brain image and the positive T-tests map to see the differences between nonrobust BPM and robust BPM. To evaluate the differences, we enlarged the area and plotted the data set for one voxel, illustrating clear that the robust BPM solution correctly discounted outliers while the nonrobust BPM did not.

5. CONCLUSIONS

In this study, we incorporated robust regression (M-estimates) into BPM to replace ordinary Least Squares estimates, and used robust variance to perform a robust hypothesis test. The results of the single voxel model show that the estimated parameters and statistical inference are not affected by outliers. Based on the simulation data, we can see that the robust regression is effective, as well as the robust inference. Therefore, this statistical method can be applied to the BPM tool box to create a robust BPM module.

The robust BPM tolerates outliers by using robust regression, which makes the tool more reliable. In practical use, the assessment of structure-function relationships will likely involve the presence of outliers. The results provided here demonstrate that robust BPM is successful in the presence or absence of outliers. The improvement in BPM solves the problem causing by outliers and provides a reliable way to quantify predictions of the relationship between structure and function of human brain.

ACKNOWLEDGEMENTS

This project was supported by NIH/NINDS 1R01NS056307 and NIH/NINDS 1R21NS064534. This work described herein has not been submitted elsewhere for publication or presentation.

REFERENCES

- [1]. Honey CJ, et al. Can structure predict function in the human brain? *NeuroImage*. 2010; 52(3): 766–776.
- [2]. Rubinov M, Sporns O, van Leeuwen C, Breakspear M. Symbiotic relationship between brain structure and dynamics. *BMC Neuroscience*. 2009; 10(55)
- [3]. Friston KJ, Ashburner JT, Kiebel SJ, Nichols TE, Penny WD. *Statistical Parametric Mapping*. 2007
- [4]. Casanova R, S R, Baer A, Laurienti PJ, Burdette JH, Hayasaka S, Flowers L, Wood F, Maldjian JA. Biological parametric mapping: a statistical toolbox for multimodality brain image analysis. *NeuroImage*. 2007; 34(1):137–143. [PubMed: 17070709]
- [5]. Chen, C. Robust Regression and Outlier Detection with the ROBUSTREG Procedure; the Twenty-seventh Annual SAS Users Group International Conference; Cary, NC: SAS Institute Inc. 2002;
- [6]. Huber PJ. Robust Estimation of a Location Parameter. *Ann. Math. Statist.* 1964; 35(1):73–101.
- [7]. Fox, J. *An R and S-PLUS Companion to Applied Regression*. 2002. Robust Regression.
- [8]. Press, WH.; T, SA.; Vetterling, WT.; Flannery, BP. *Numerical recipes: the art of scientific computing*. Third ed.. 2007.
- [9]. Beaton AE, Tukey JW. The fitting of power series, meaning polynomials, illustrated on band-spectroscopics data. *Technometrics*. 1974; 16:147–185.
- [10]. Holland PW, Welsh RE. Robust regression using iteratively reweighted least-squares. *Communications in Statistics - Theory and Methods*. 1977; 6(9):813–827.
- [11]. Street JO, Carroll RJ, Ruppert D. A Note on Computing Robust Regression Estimates via Iteratively Reweighted Least Squares. *The American Statistician*. 1988; 42:152–154.
- [12]. Huber, PJ. *Robust Statistics*. John Wiley & Sons, Inc.; Hoboken, NJ: 1981.
- [13]. Huber PJ. Robust Regression: Asymptotics, Conjectures and Monte Carlo. *The Annals of Statistics*. 1973; 1(5):799–821.
- [14]. Dumouchel, W.; O'Brien, F. *Computing and graphics in statistics*. Springer-Verlag New York, Inc.; New York, NY, USA: 1992. Integrating a robust option into a multiple regression computing environment; p. 41-48.

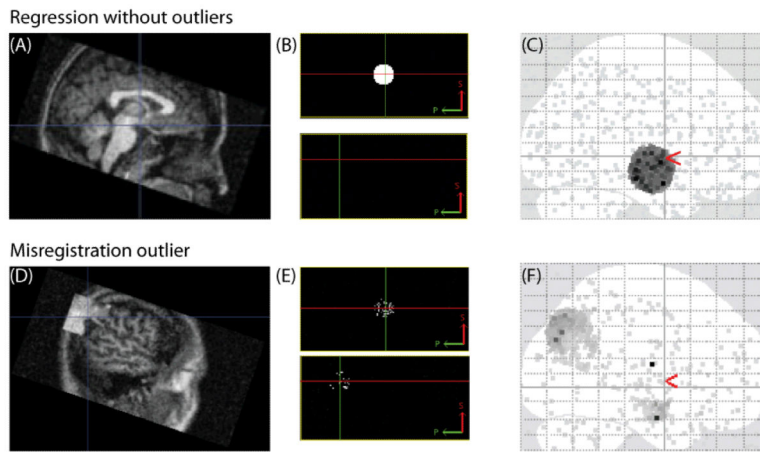


Figure 1. Impact of outliers in BPM. (A) is one of the regressor images without outliers. The main modality images are: $Y = 3X$ inside a spherical region, $Y = \text{constant}$ outside the region. (B) is the Beta estimation when there are no outliers. (C) is the significant results when there are no outliers, (D) is the shifted regressor image, the center cube shifts to another region. The center cube of the paired main modality image shifts to the same region. (E) is the estimated Beta from original BPM when there are outliers. (F) is the significant results from original BPM when there are outliers.

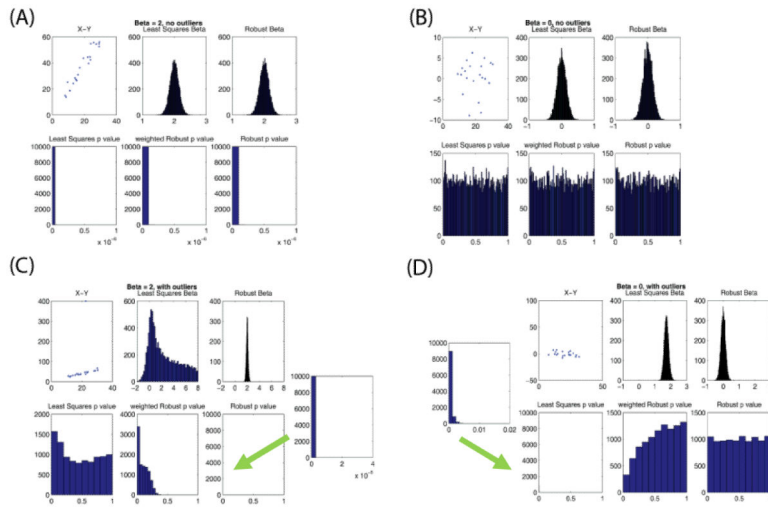


Figure 2. Robust regression in one voxel. The model is $y = \beta x + \eta$. Null hypothesis is $H_0: \beta = 0$. (A) shows the histogram of estimated Beta and p value from ordinary least squares estimates and robust estimates when $\beta = 2$ and there are no outliers. All β estimations are around 2, and p values are significant. (B) shows the histogram of estimated β and p value when $\beta = 0$ and there are no outliers. All β estimations are around 0, and p values are not significant. (C) shows the histogram of estimated β and p value when $\beta = 2$, and there are outliers. (D) shows the histogram of estimated β and p value when $\beta = 0$ and there are outliers.

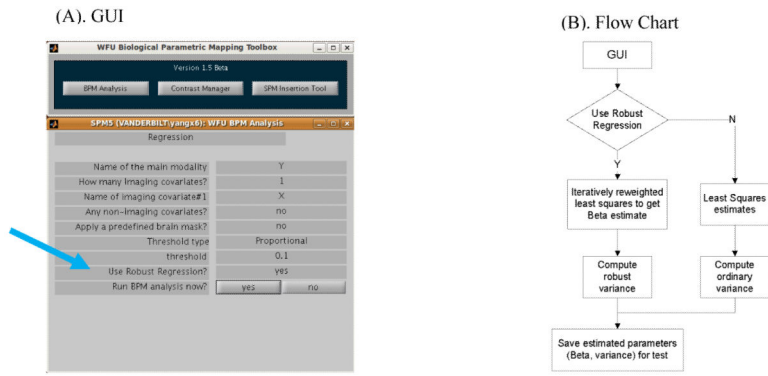


Figure 3. Modified parts in BPM. (A) is the GUI in BPM analysis, where we added a choice between robust regression and least squares estimates. B shows the flowchart of the program where we incorporated robust regression.

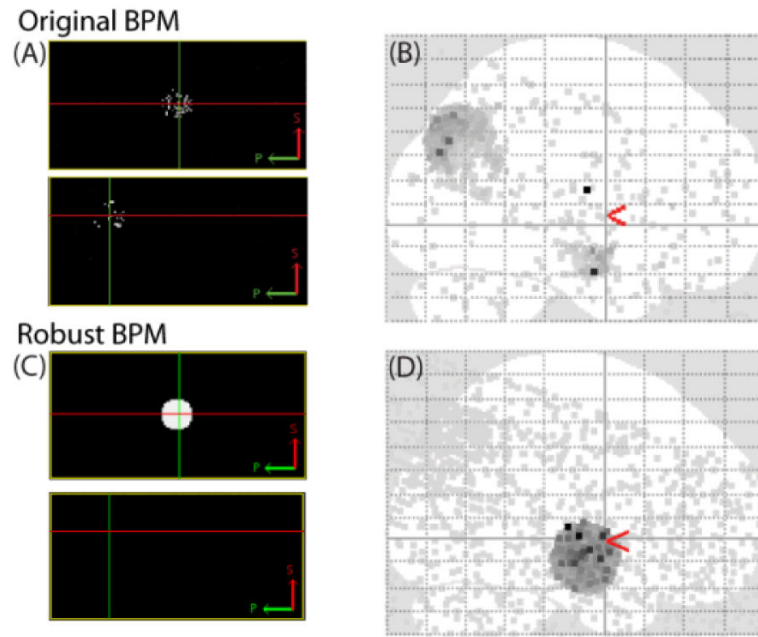


Figure 4. Results from robust BPM with outliers. (A) is the estimated β from original BPM. (B) is the significant results from original BPM. (C) shows the estimated β from robust BPM, it is exactly the ideal β . (D) is the significant results from robust BPM, though it is not exactly the same as the results when there are no outliers in original BPM, we can see significance inside the spherical region, and less significance outside the region.

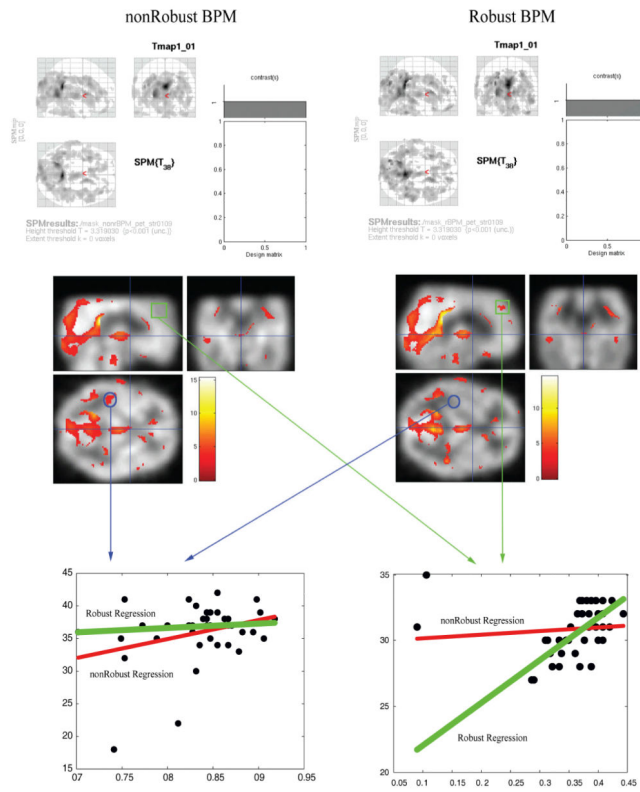


Figure 5. Regression of empirical Data. Gray matter structure data of twenty participants from year 1 and year 9 (40 images) were regressed on the PET data. The two plots are the data for one voxel. The x axis shows the value of Gray matter structure data and the y axis shows the value of PET data. The red line is the fit of the non robust regression while the green line is the fit of the robust regression.